



A fluorescence turn-on probe for hydrogen sulfide and biothiols based on PET & TICT and its imaging in HeLa cells

Xueqiong Zhang^a, Xiaodong Jin^{a,b}, Caiting Zhang^a, Hui Zhong^{c,*}, Hongjun Zhu^{a,*}

^a Department of Applied Chemistry, College of Chemistry and Molecular Engineering, Nanjing Tech University, Nanjing 211816, China

^b Department of Criminal Science and Technology, Jiangsu Police Institute, Nanjing, Jiangsu 210031, China

^c Jiangsu Key Laboratory for Chemistry of Low-Dimensional Materials, School of Chemistry and Chemical Engineering, Huaiyin Normal University, Huaian 223300, China

ARTICLE INFO

Article history:

Received 30 June 2020

Received in revised form 1 August 2020

Accepted 10 August 2020

Available online 17 August 2020

Keywords:

Chalcone

ESIPT

PET

Hydrogen sulfide

Biothiols

HeLa cells

ABSTRACT

In this paper, a photoinduced electron transfer (PET)& twisted intramolecular charge transfer (TICT)-based fluorescent probe (**1**) for detecting biothiols (GSH/Cys/Hcy) and hydrogen sulfide with fluorescence turn on was developed. The probe could recognize hydrogen sulfide over primary ions and selectively detect GSH/Cys/Hcy over other amino acids with fluorescence turn-on (an ESIPT process). H₂S can be distinguished from GSH/Cys/Hcy with wavelength shift by UV-Vis spectra. In addition, detection limits for H₂S/GSH/Cys/Hcy of probe **1** were 1.42 μM (0–100 μM), 0.13 μM (0–40 μM), 0.27 (0–30 μM), 0.22 μM (0–40 μM), respectively. The proposed thiolysis of the 2,4-dinitrochlorophenyl ether reaction in identification process was verified by the characteristic peak in ¹H NMR and HRMS spectra. Finally, the biological imaging experiments and low cytotoxicity investigations in HeLa cells demonstrated that probe **1** could provide a promising method for the determination of H₂S and biothiols in aqueous solution and living cells.

© 2020 Published by Elsevier B.V.

1. Introduction

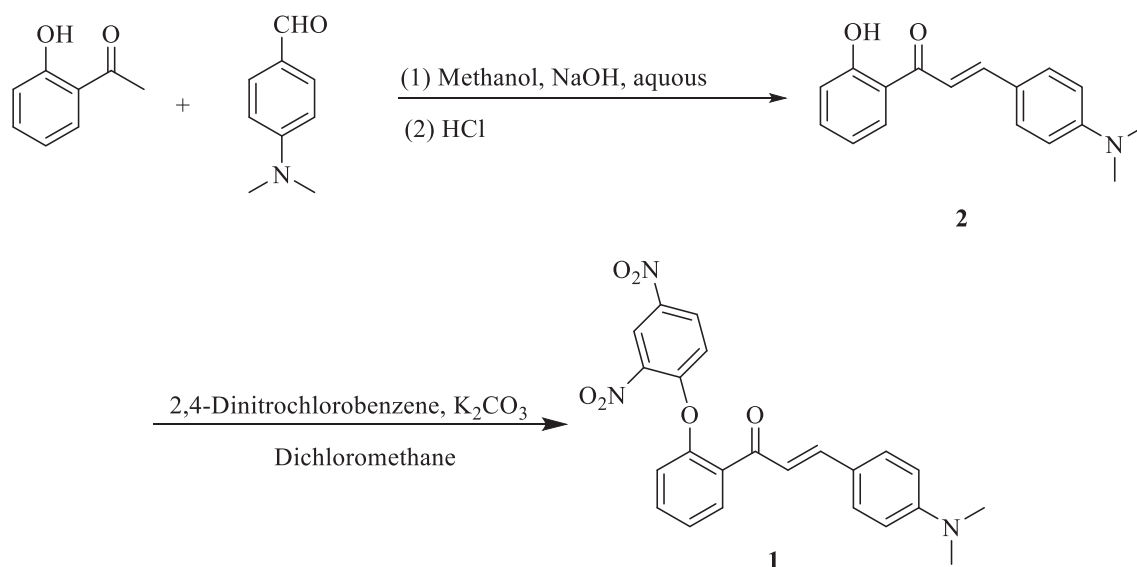
As well known, hydrogen sulfide [1–3] plays many vital roles in physiological and pathological processes. As an intracellular gas transmitter, H₂S is useful in protecting heart and relaxing muscles with 50–160 μM in the central nervous system and 10–100 μM in blood [7,8]. The abnormal H₂S level in vital organs may induce Down's syndrome, Alzheimer's disease and diabetes [9,10]. Biothiols [4–6] also occupy important positions in the series of vital processes. For example, glutathione (GSH) is the most abundant biothiol with concentration at 2–20 μM in extracellular fluid and 2–10 mM in intracellular fluid, and it acts an antioxidant to against toxins and free radicals. Exceptional GSH level is related to Alzheimer's, diabetes, liver damage, cancers and HIV infection [11,12]. Cysteine (Cys) can contribute in detoxification, immunological competence, growth and protein synthesis at 3–200 μM. Deficiency of Cys has been proved to be linked to liver damage, brain damage, hair loss, skin lesions and weakness [13–15]. Homocysteine (Hcy) can promote cell proliferation and produce GSH with concentration of 5–15 μM. Excessive Hcy level (>15 μM) has been reported to be associated with myocardial infarction, stroke, venous thromboembolism, vascular disease and Alzheimer's [16,17]. Therefore, it is still a hot topic to detect and analyze hydrogen sulfide and biothiols sensitively and selectively in biotics and physiology [18–21].

The current techniques for H₂S and biothiols include photoluminescence, electrochemical, colorimetry, chromatography, mass spectrometry and et al. [3,22–26]. When compared with other detection techniques, fluorescent probes [27–30] have been reported for photoluminescence materials which were performed excellently in sensitivity, selectivity, simplicity, and operability. The special reaction between fluorescent probes and mercapto compounds include nucleophilic substitution by thiol [31,32], cleavage reaction by mercapto group [10,33], Michael addition [34], reduction reaction [35,36], thiolysis reaction and et al. GSH/Cys/Hcy and H₂S have the similar mercapto structural characteristics, so it is demanding to detect and discriminate them [37,38]. On the other hand, it is still a challenge to provide a single probe which could simultaneously distinct GSH/Cys/Hcy and H₂S from the new insight into multifaceted biological interaction.

The excited-state intramolecular proton transfer (ESIPT)-based dyes [39–41] have been applied to design fluorescent probes for sensing anions, cations, and small molecules [41–44] in situ and vivo due to its advantages like redder emission, larger Stock's shift and fluorescence turn-on. It has been reported [41,45] that chalcone (compound **2**) is an ESIPT-active dye with red-emitting, this molecule has advantages like easy synthesis, stable optical properties, hupotoxicity and et al. Inspired by these virtues, chalcone was chosen as the fluorophore to construct probe **1**. Equipped with 2,4-dinitrochlorophenyl group as the receptor, probe **1** presented fluorescence quenching by intramolecular PET&TICT process. Probe **1** showed fluorescence turn on by an ESIPT process after the thiolysis of the 2,4-dinitrochlorophenyl ether by H₂S/thiols. And the

* Corresponding authors.

E-mail addresses: huizhong@hytc.edu.cn (H. Zhong), zhuwj@njtech.edu.cn (H. Zhu).



designed probe (**1**) showed high sensitivity and selectivity over other primary ions and amino acids in the physiological environment. In addition, probe **1** could sense H₂S in HeLa cells and had been proved low cytotoxicity in HeLa cells, MCF-10A and MCF-7 cells. All the results predict probe (**1**) is a promising detection tool for H₂S and biothiols (GSH/Cys/Hcy).

2. Experimental

2.1. Materials and instrumentations

All chemicals used in this paper were obtained from Tansoole without further purification. Silica gel (300–400 mesh, Qingdao Haiyang Chemical Co.) was used for column chromatography. Dichloromethane was processed with CaH₂ and stored with 4 Å molecular sieves.

¹H NMR, and ¹³C NMR spectra were measured on a Bruker AV-400 spectrometer with chemical shifts reported in ppm (in CDCl₃ or d₆-DMSO, TMS as internal standard). UV-Vis spectra were acquired on a Hewlett-Packard 8453 diode-array spectrometer. All fluorescence measurements were recorded on a Hitachi-F-4600 fluorescence spectrophotometer. HI 2221 calibration check pH/ORP meter was used to measure the pH of phosphate buffer.

2.2. Synthesis

Synthesis of 2'-hydroxy-4-(dimethylamino)chalcone (**2**). Compound **2** was carried out according to the literature methods [44–47] as a purplish solid.

Synthesis of 2'-((2,4-dinitro-phenoxy)-4-(dimethylamino) chalcone (**1**). 2,4-Dinitrochlorobenzene (243 mg, 1.2 mmol), and compound **2** (267 mg, 1.0 mmol) was dissolved in 30 mL anhydrous dichloromethane under N₂ atmosphere, then K₂CO₃ (138 mg, 1.0 mmol) was added. The mixture was stirred at 30 °C for 12 h. The solution was concentrated under reduced pressure and the product was purified using silica gel chromatography (petroleum ether: ethyl acetate = 10: 1 to 3: 1, v/v) to afford compound **1** as an orange solid (220 mg, yield: 51%). ¹H NMR (400 MHz, CDCl₃) δ 8.80 (d, *J* = 2.7 Hz, 1H), 8.26 (dd, *J* = 9.3, 2.7 Hz, 1H), 7.84–7.77 (m, 1H), 7.61 (dd, *J* = 7.7, 1.5 Hz, 1H), 7.53–7.39 (m, 4H), 7.20 (d, *J* = 8.1 Hz, 1H), 7.06 (d, *J* = 15.6 Hz, 1H), 6.89 (d, *J* = 9.3 Hz, 1H), 6.65 (d, *J* = 8.9 Hz, 2H), 3.04 (s, 6H). ¹³C NMR (100 MHz, CDCl₃) δ 190.30, 156.51, 152.41, 150.67, 141.26, 138.56, 133.89, 132.97, 131.21, 130.95, 129.01, 127.17, 122.24, 122.06, 121.78, 119.36, 118.06, 111.75, 77.37, 77.06, 76.74. HRMS (ESI, *m/z*) calcd for C₂₃H₂₀N₃O₆⁺ [M + H]⁺: 434.13466, found: 434.13431 (Scheme 1).

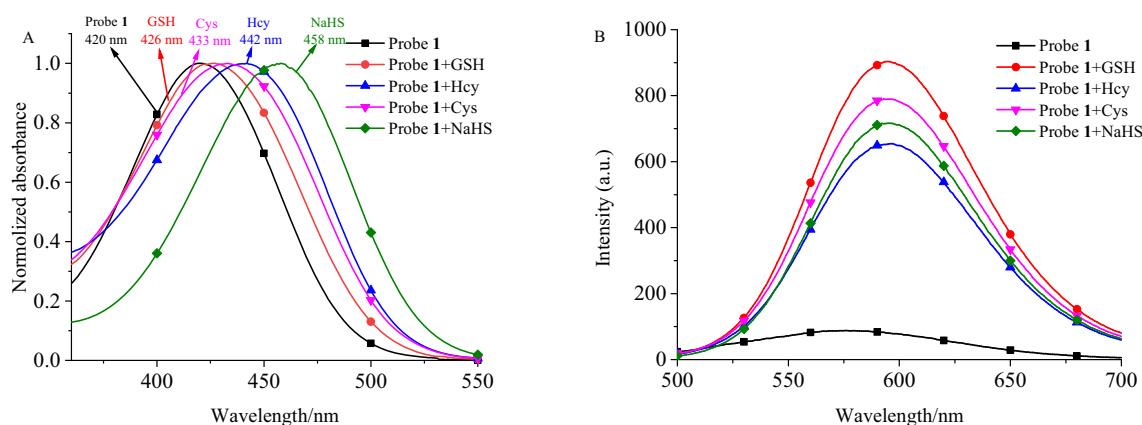
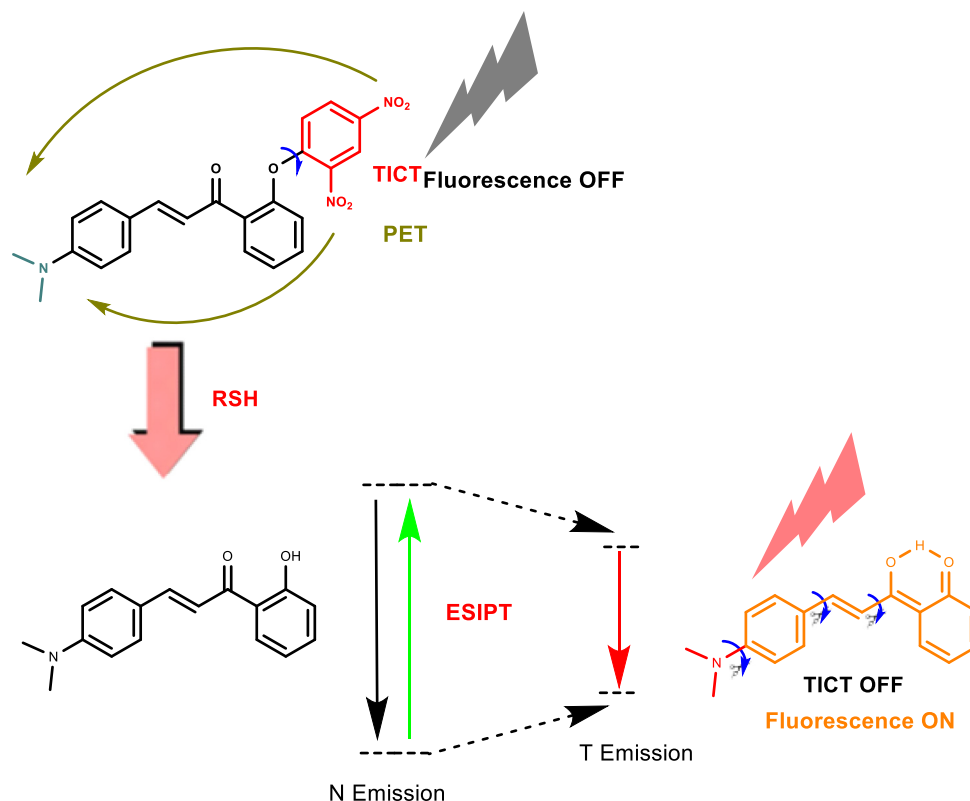


Fig. 1. (A) Absorption spectra of probe **1** (50 μM) in the absence and presence of NaHS/GSH/Cys/Hcy (500 μM) in DMSO. (B) Fluorescence spectra of probe **1** (50 μM) toward NaHS/GSH/Cys/Hcy (500 μM). λ_{ex} = 480 nm, d_{ex} = 5 nm, d_{em} = 5 nm.



Scheme 2. Luminous mechanism of probe 1 and compound 2.

3. Results and discussion

3.1. UV-Vis and fluorescence measurements for probe 1 toward NaHS and thiols

Fig. 1(A) displayed the maximum absorption of probe 1 (50 μM) at 420 nm in DMSO at room temperature. Upon adding NaHS or biothiols, new absorption bands appeared and centered at 458 nm (NaHS), 426 nm (GSH), 433 nm (Cys) and 442 nm (Hcy), respectively. Hence, H_2S and GSH/Cys/Hcy can be distinguished by the absorption spectra. In the emission spectra, probe 1 behaved a weak emission peak at 575 nm (as shown in Fig. 1(B), $\lambda_{\text{ex}} = 480$ nm), which might be due to a photoinduced electron transfer (PET) process with the 2,4-dinitrophenyl moiety acting as the electron acceptor, and *N,N*-dimethylaniline group as the electron donor (as seen in Scheme 2). After adding NaHS and GSH/Cys/Hcy, the maximum emission of probe 1 red-shifted to 600 nm with obvious fluorescence enhancement, which may be attributed to transformation between the normal form and keto form of compound 2, respectively. The generation of compound 2 could be ascribed to the thiolysis of H_2S and the thiol-induced nucleophilic substitution and rearrangement reaction. All these results demonstrate that probe 1 has the potential for being an efficient spectroscopic probe for H_2S and biothiols (GSH/Cys/Hcy).

For evaluating the application of probe 1 in physiological condition, water content experiment and pH-response experiment were carried out by fluorospectro photometer. The fluorescent intensity of probe 1 nearly unchanged with variation of water content and pH value. While, water content reduction caused intensity increasing after reacting with NaHS (see Fig. S1). This may be ascribed the excessive water proportion would induce solid aggregated, therefore 50% water content was selected in the spectra test. As seen in Fig. 2, the probe 1 behaved stably in DMSO-PBS solution with weak acid, however, neutral, weak base, and the strong base would disturb the detection effect. In

addition, the fluorescence intensity of probe 1 at 600 nm in DMSO-PBS solution (5:5, v/v, pH = 7.40) remained stable for 0–72 h (as shown in Fig. S2). Obviously, probe 1 performs high stability and ought to be an applicable tool in physiological.

Next, the time-dependent experiment was studied to monitor the reaction dynamics between probe 1 (50 μM) and NaHS/GSH/Cys/Hcy in DMSO-PBS (5:5, v/v, pH = 7.02, 12.5 mM) to evaluate the detection time of reaction-based probes. Upon the addition of 10 equiv. of NaHS/GSH/Cys/Hcy, respectively, the emission intensity of probe 1 at 600 nm increased gradually due to the ESIP progress (Fig. 3). And the

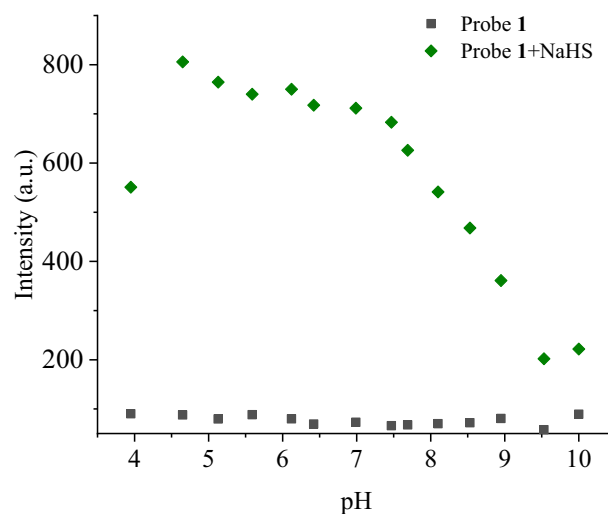


Fig. 2. Fluorescence spectra ($\lambda = 600$ nm) of probe 1 (50 μM) upon addition of 10 equiv. of NaHS at different pH values in DMSO-PBS (5:5, v/v).

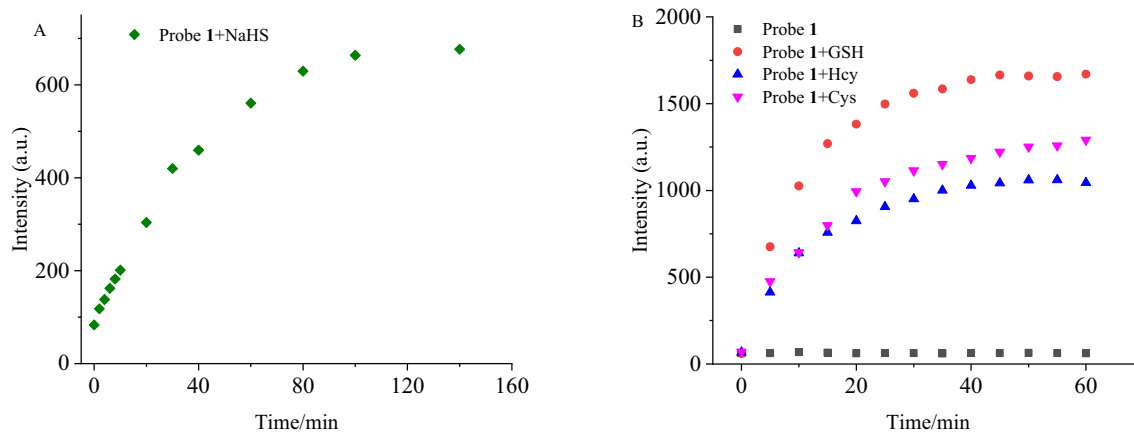


Fig. 3. Time-dependent fluorescence intensity ($\lambda = 600$ nm) changes of probe **1** ($50 \mu\text{M}$) upon addition of 10 equiv. of NaHS (A) and GSH/Cys/Hcy (B) in DMSO-PBS (5:5, v/v, pH = 7.40, 12.5 mM) at room temperature.

fluorescence intensity reached an optical stabilization platform after 100 min with NaHS, and 60 min with biothiols (GSH/Cys/Hcy), respectively.

3.2. Sensitive optical response of probe **1** toward H_2S and biothiols

Titration experiments were carried out by gradually adding NaHS to evaluate the quantitative analysis of probe **1**. The emission spectra were collected after reacting completely. As shown in Fig. 4, the fluorescent intensity at 600 nm was gradually enhanced with the addition of NaHS, and exhibited an excellent linear relationship of emission intensity with NaHS concentration (0–100 μM) in the DMSO/PBS (5:5, v/v) solution ($R^2 = 0.9926$). These concentrations are well within the range that has been used to elicit physiological responses. The detection limit was 1.42 μM based on $3\sigma/k$ (where σ is standard deviation of the blank solution for 20 samples, and k is the slope of the calibration curve).

Next, the thiolysis sensitivity of probe **1** toward different biothiols (GSH, Cys, and Hcy) was also investigated to evaluate the quantitative analysis of probe **1**. It was found that there was an obvious fluorescence turn-on after addition of amounts of GSH/Cys/Hcy at 600 nm. As shown in Fig. 5, the fluorescent intensity showed a good linear relationship with GSH/Cys/Hcy in the DMSO/PBS (5:5, v/v) solution. The linear range are 0–40 μM for GSH ($Y = 87.0105 + 21.8200X$, $R^2 = 0.9965$), 0–30 μM for Cys ($Y = 71.4216 + 10.7624X$, $R^2 = 0.9923$), 0–40 μM for Hcy ($Y = 78.0580 + 13.3572X$, $R^2 = 0.9939$), respectively. The detection limits of GSH, Cys, and Hcy were calculated to be 0.06 μM ,

0.12 μM , 0.10 μM , respectively. The valid analyzing ranges of GSH/Cys/Hcy are within the physiological ranges. The sensitivity tests indicated that the chemodosimeter (probe **1**) could detect biothiols (GSH/Cys/Hcy) quantitatively at the physiological level by the fluorescence spectroscopy method.

To assess the possibility of simultaneous detection for H_2S and GSH/Cys/Hcy, the UV-Vis and fluorescence of mixture of H_2S and GSH with probe **1** were investigated. Keeping the total concentrations of H_2S and GSH consistent, as the $[\text{H}_2\text{S}]/[\text{GSH}]$ ratio increased, the maximum absorption wavelength red-shifted from 426 nm to 458 nm with absorption increased (Fig. S3). In addition, as the $[\text{H}_2\text{S}]/[\text{GSH}]$ ratio increased, the fluorescence intensity gradually decreased with a linear response (Fig. S4, $R^2 = 0.9924$). Therefore, the concentration of H_2S can be measured by UV-Vis absorption at 458 nm, and the concentration of GSH can be determined by emission intensity at 600 nm. Take advantages of UV-Vis and emission spectra, probe **1** can detect GSH and H_2S quantitatively when they coexist, probe **1** would be a potential tool in biological samples.

3.3. Selective optical response of probe **1** to various analytes and amino acids

To evaluate the selectivity of probe **1** for NaHS, the fluorescence spectra with sulfides (like $\text{S}_2\text{O}_3^{2-}$, SO_3^{2-} , GSH, Hcy, Cys, $\text{S}_2\text{O}_8^{2-}$, HSO_3^-), cations (Cr^{3+} , Al^{3+} , Zn^{2+} , Ni^{2+} , Mn^{2+} , etc) and anions (ClO_4^- , I^- , Br^- , Cl^- , H_2PO_4^- , PO_4^{3-} , etc) were tested. As shown in Fig. 6(A), **1** displayed negligible changes in emission intensity (at 600 nm) upon adding 10

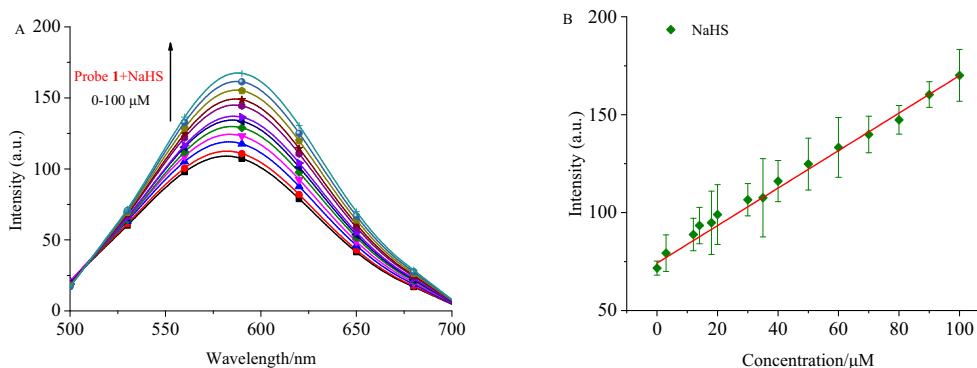


Fig. 4. (A) Fluorescence spectra of probe **1** ($50 \mu\text{M}$) upon adding NaHS (0–100 μM). (B) The fluorescence intensity ($\lambda = 600$ nm) of probe **1** were linearly related to the concentration of NaHS (0–100 μM) ($R^2 = 0.9926$, $\text{CDL} = 0.43 \times 3/0.91 = 1.42 \mu\text{M}$).

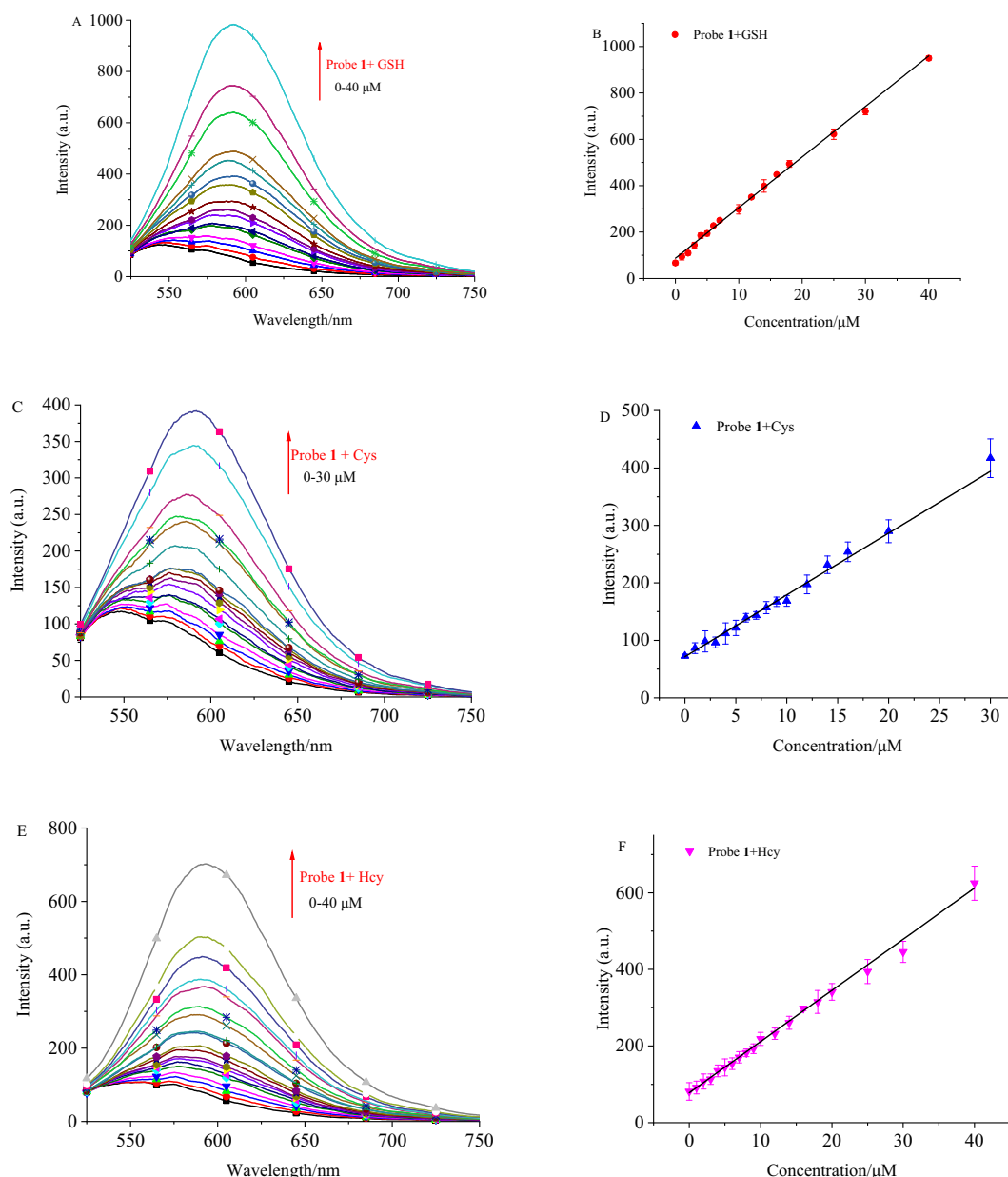


Fig. 5. Titration fluorescence spectra of probe **1** (50 μM) upon addition of 10 equiv. of GSH (A, B), Cys (C, D), and Hcy (E, F) and intensity ($\lambda = 600$ nm) of probe **1** (50 μM) upon addition of biothiols in DMSO-PBS (5:5, v/v, pH = 7.40, 12.5 mM) at room temperature.

equiv. of these interfering analytes except H₂S, GSH, Hcy, and Cys. The competitive experiments showed the fluorescent detection of H₂S was obstructed by metal ions (Zn²⁺, Cd²⁺, Hg²⁺) due to their complexation toward S²⁻. Zn²⁺ is a kind of essential trace elements [48–51] in living body, its interference in H₂S detection needs to be taken seriously. Meanwhile, according to the K_{sp} of ZnS, the concentrations of Zn²⁺ in physiological condition is too low to interfere the H₂S detection and not enough to influence biological test when H₂S and Zn²⁺ coexist. Moreover, Cd²⁺ and Hg²⁺ are heavy metal ions, they are generally not presented in living body. Therefore, the three metal ions (Zn²⁺, Cd²⁺, Hg²⁺) are negligible to disturb the H₂S detection. These results could suggest other species caused insignificant effects on H₂S detection.

Next, probe **1** was subject to react with amino acids (Arg, Trp, Ile, Pro, etc) that have a hydrosulfonyl and the structures were similar to GSH/Hcy/Cys. The addition of 10 equiv. of amino acids exhibited almost no changes with probe **1** in emission behaviour (Fig. 6(B), red column). As seen in Fig. 6(B) (green, dark blue, and cerulean column), the

competitive experiments were also investigated by adding respective biothiols (GSH/Hcy/Cys) to the mixture solution of probe **1** with amino acids. The results indicated that the detection of GSH/Cys/Hcy could survive possible interference from amino acids. All the results demonstrated that probe **1** possesses a high selectivity toward hydrogen sulfide and biothiols (GSH/Hcy/Cys).

3.4. Mechanism verification of probe **1** for H₂S

To validate the posed detection mechanism for H₂S, the ¹H NMR spectra of probe **1** in d₆-DMSO with or without NaHS at room temperature (Fig. 7) were tested. The hydroxyl hydrogen Ha (at ~13.20 ppm) and aromatic proton Hb (at ~8.30 ppm), Hc (at ~6.95 ppm) and Hd (at ~6.75 ppm) appeared after adding NaHS in probe **1** solution, this phenomenon indicated the cleavage of ether bond. The released fluorophore compound **2** was also found by HRMS (calcd for [M + H]⁺: 268.13321, found: 268.13348, Fig. S5). In addition, the

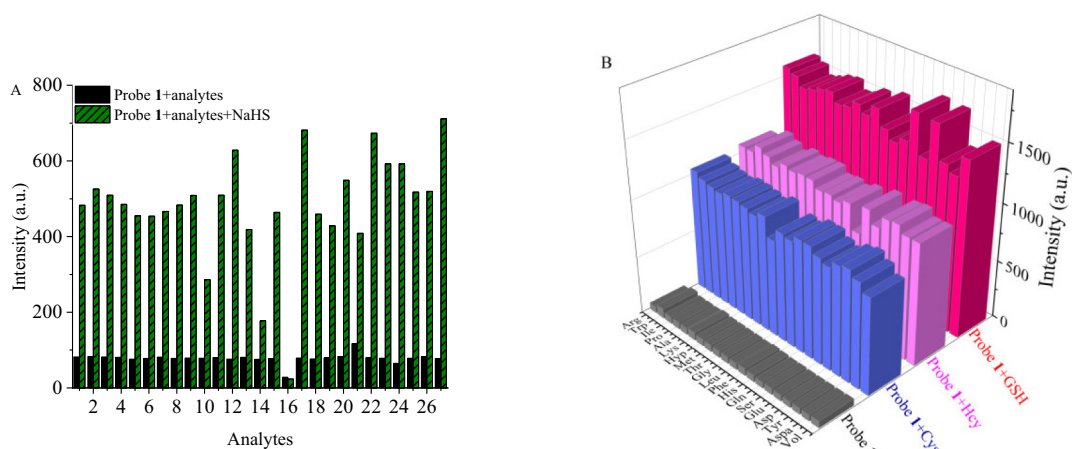


Fig. 6. (A) Represents the addition of NaHS to the above analyte-containing solutions (bars show: 1. ClO_4^- , 2. I^- , 3. Br^- , 4. Cl^- , 5. H_2PO_4^- , 6. PO_4^{3-} , 7. HSO_4^- , 8. Cl^{3+} , 9. Al^{3+} , 10. Zn^{2+} , 11. Ni^{2+} , 12. Mn^{2+} , 13. Fe^{3+} , 14. Cd^{2+} , 15. Mg^{2+} , 16. Hg^{2+} , 17. Thiourea, 18. Et_3N , 19. Ethylenediamine, 20. $\text{S}_2\text{O}_3^{2-}$, 21. SO_3^{2-} , 22. GSH, 23. Hcy, 24. H_2O_2 , 25. *t*-BuOOH, 26. $\text{S}_2\text{O}_8^{2-}$, 27. NO_2^- , 28. HSO_3^- , 29. Cys, 30. blank). (B) Represents the addition of GSH/Cys/Hcy to the amino acids.

wavelengths changed in UV-Vis spectra can be ascribed to the formation of **1**-GSH, **1**-Cys and **1**-Hcy in recognition process (Fig. S6) when responded to GSH/Cys/Hcy, and they had been verified by HRMS (Fig. S7).

3.5. Theoretical calculation

To better understand the luminous mechanism, probe **1** and compound **2** were examined by density function theory (DFT). As seen in

Fig. 8, the electron density localizes on the 2, 4-dinitrophenyl group in the lowest unoccupied molecular orbital (LUMO) and the π electrons focused on the *N,N*-dimethylaniline group in the highest occupied molecular orbital (HOMO), we suppose it could be corresponded with PET [52,53] of probe **1**. And the intramolecular rotation of 2, 4-dinitrophenyl group in probe **1** (Fig. S8) is 67.6° , which is helpful to result in fluorescence quenching with TICT pattern [54,55]. While, the electron intensity in the HOMO and LUMO of compound **2** spread over the whole skeleton and the molecule structure is in the same plane

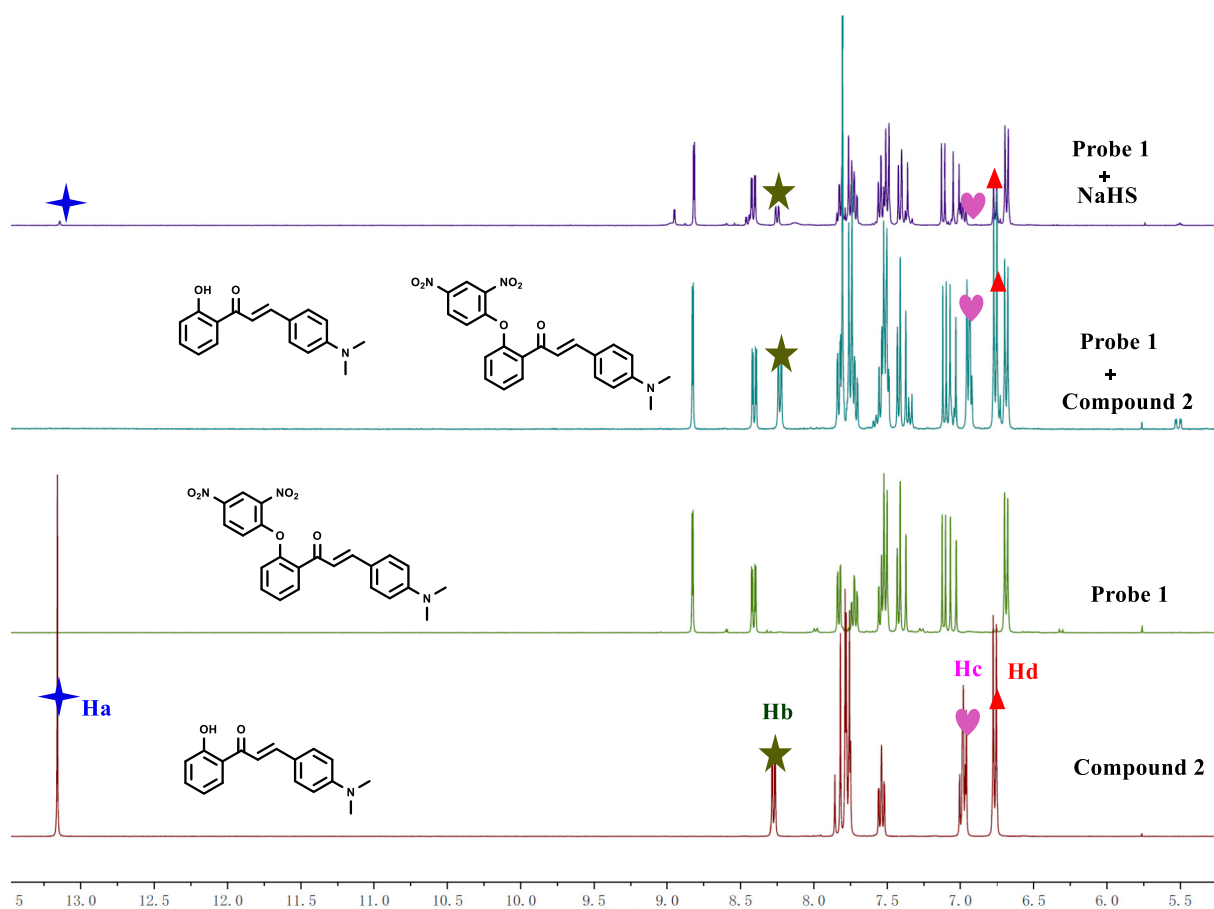


Fig. 7. The ^1H NMR spectra of probe **1** + NaHS, probe **1** + compound **2**, probe **1** and compound **2** only in d_6 -DMSO. $[\mathbf{1}] = [\mathbf{2}] = 4.0 \times 10^{-2}$ M, $[\text{NaHS}] = 4.0 \times 10^{-1}$ M.

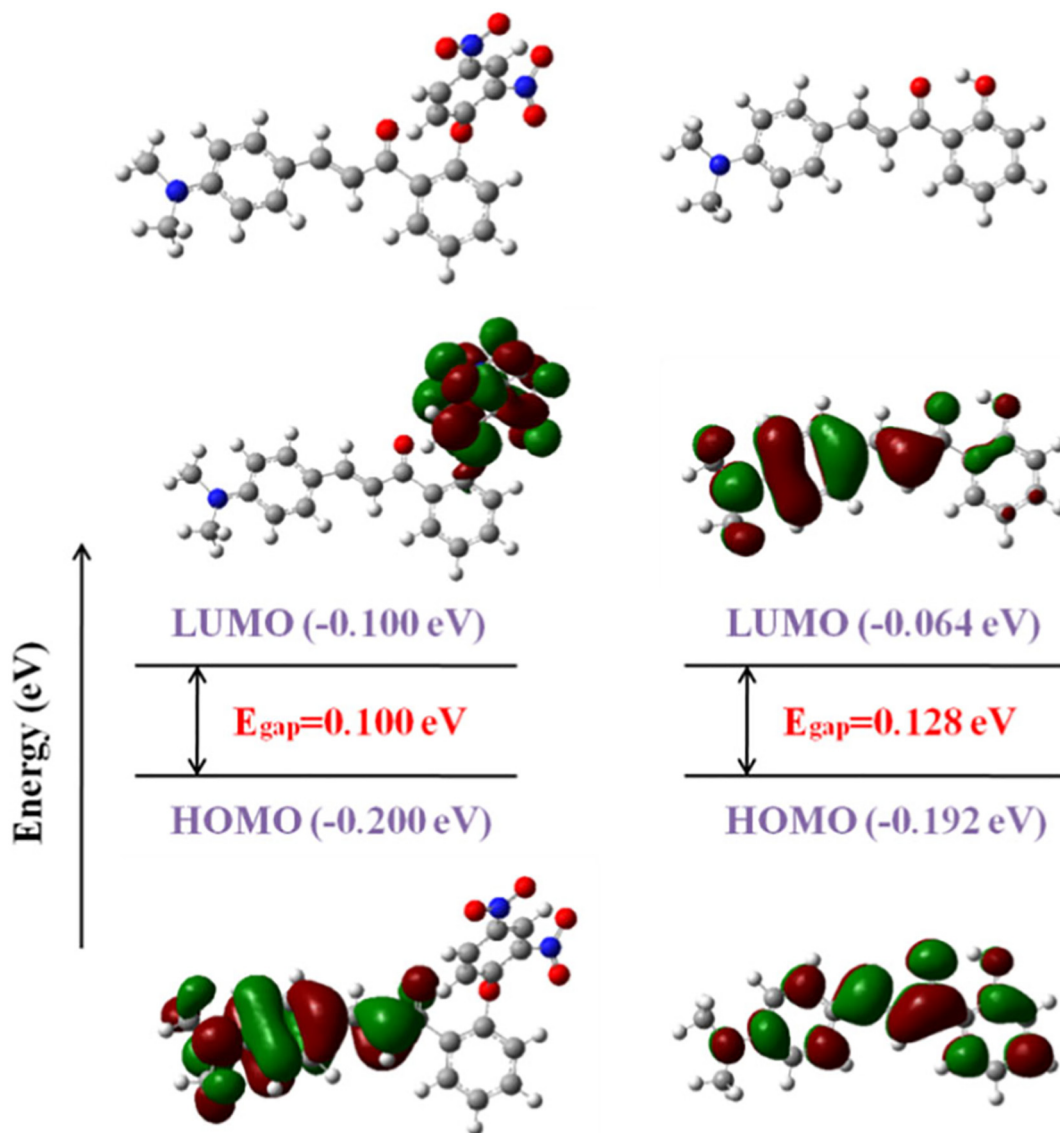


Fig. 8. Structural optimization and HOMO, LUMO orbitals of probe **1** and compound **2** by B3LYP/6-31G*.

which disturbed the TICT process. In addition, the alkenyl group and keto is an excellent condition to form ESIPT form [38,56]. All these results make the recognition process showing a fluorescence turn-on. The predicted mechanism of probe **1** toward RSH has been presented in Fig. 9.

3.6. Imaging of probe **1** in living cells

The above solution experiments revealed that probe **1** could detect with high selectivity and sensitivity. In addition, the potential application of probe **1** in HeLa cells was examined, and probe **1** (50 μM) showed quite weak fluorescence (Fig. 9A) after incubating with HeLa cells for 30 min at 37 $^{\circ}\text{C}$, the weak fluorescence revealed that probe **1** has successfully infiltrated the living cells for intracellular H_2S /biothiols (Fig. S9). Next, the HeLa cells were continuously incubated with 200 μM and 500 μM NaHS, for another 2.5 h. Then, an obvious fluorescence intensity increase in HeLa cells (Fig. 9B and C) was observed, which were attributed to the release of compound **2** via the thiolysis of ether linkage. Moreover, the cytotoxicity of probe **1** was assessed with various living cells (HeLa cells, MCF-7, MCF-10A, Fig. S10–12) by MTT assays, the results presented that probe **1** has quite low cell

cytotoxicity. These results showed the developed probe **1** has the ability as an excellent detecting tool to recognize H_2S in living cells.

4. Conclusion

In this paper, a chalcone-probe (**1**) on the basis of 2, 4-dinitrophenyl ether reaction has been synthesized and characterized. Probe **1** shows a distinct fluorescence turn-on after adding H_2S /GSH/Cys/Hcy by the transformation from PET&TICT to ESIPT. Probe **1** possesses a high selectivity and sensitivity toward both H_2S and GSH/Cys/Hcy. Furthermore, the application of probe **1** in HeLa cells indicates that probe **1** has great potential for hydrogen sulfide and biothiols (GSH/Cys/Hcy) in biology and pathology.

CRediT authorship contribution statement

Xueqiong Zhang: Methodology and Synthesis, Optical measurement and data analyses, Writing- Original draft preparation;

Xiaodong Jin: Supervision, Writing- Reviewing and Editing;

Caiting Zhang: Optical measurement, Writing- Reviewing and Editing;

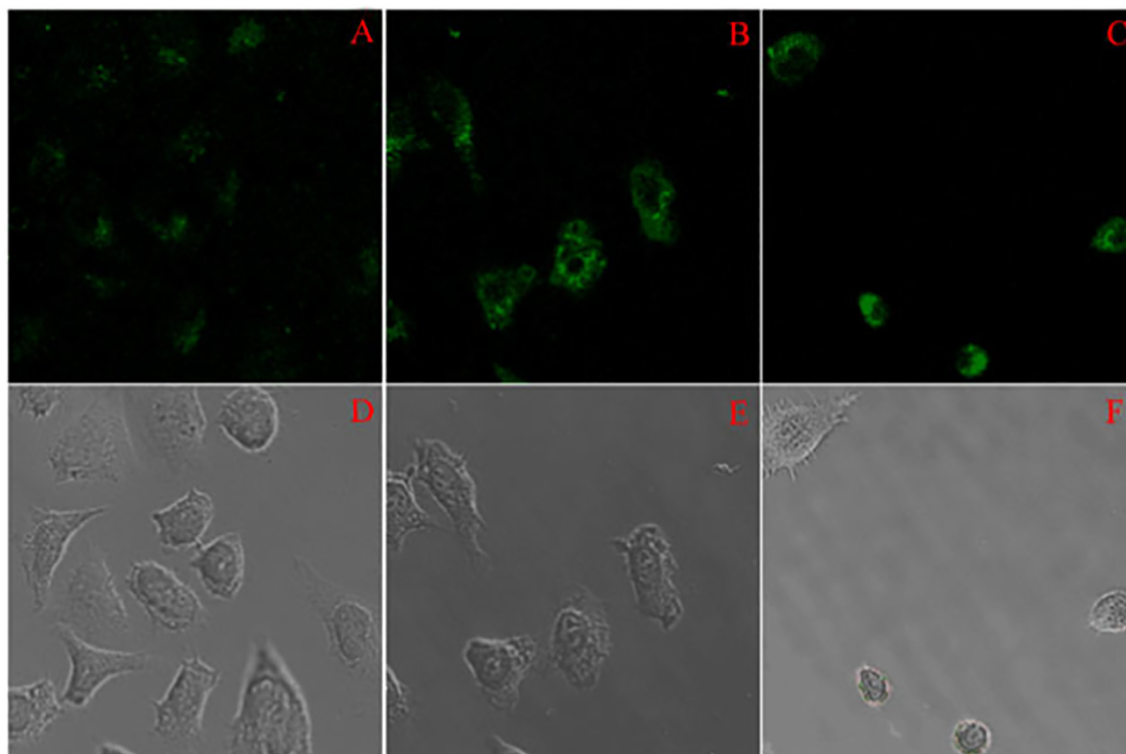


Fig. 9. Images of probe **1** (50 μM) in HeLa cells with NaHS at 37 $^{\circ}\text{C}$ for 2.5 h at green channel (A-C, A, 0 μM ; B, 200 μM ; C, 500 μM , $\lambda_{\text{ex}} = 490 \text{ nm}$), (D-F), Bright-field.

Zhong Hui: Supervision and Funding acquisition.

Hongjun Zhu: Supervision and Funding acquisition.

Declaration of competing interest

The authors declare that they have no known competing financial interests or personal relationships that could have appeared to influence the work reported in this paper.

Acknowledgements

This research was supported by the National Key Research and Development Program of China (2016YFB0301703), the National Natural Science Foundation of China (21775051, 21375044), Natural Science Foundation of Jiangsu Province (BK20191416), and the High-level Introduction of Talent Scientific Research Start-up Fund of Jiangsu Police Institute (JSPI17GKZL402).

Appendix A. Supplementary data

Supplementary data to this article can be found online at <https://doi.org/10.1016/j.saa.2020.118839>.

References

- [1] S. Singh, R. Banerjee, PLP-dependent H_2S biogenesis, *BBA-Proteins Proteom* 1814 (2011) 1518–1527.
- [2] H. Kimura, Hydrogen sulfide: its production and functions, *Exp. Physiol.* 96 (2011) 833–835.
- [3] S. Koike, K. Kawamura, Y. Kimura, et al., Analysis of endogenous H_2S and H_2S_n in mouse brain by high-performance liquid chromatography with fluorescence and tandem mass spectrometric detection, *Free Radical Bio. Med.* 113 (2017) 355–362.
- [4] O. Rusin, L.N. St, R.A. Agbaria, et al., Visual detection of cysteine and homocysteine, *J. Am. Chem. Soc.* 126 (2004) 438–439.
- [5] P.K. Pallela, T. Chiku, M.R. Carvan, D.S. Sem, Fluorescence-based detection of thiols in vitro and in vivo using dithiol probes, *Anal. Biochem.* 352 (2006) 265–273.
- [6] H. Zhang, L. Xu, W. Chen, et al., A lysosome-targetable fluorescent probe for simultaneously sensing Cys/Hcy, GSH, and H_2S from different signal patterns, *ACS Sensors* 3 (2018) 2513–2517.
- [7] B. Olas, Hydrogen sulfide in signaling pathways, *Clin. Chim. Acta* 439 (2015) 212–218.
- [8] X. Jin, S. Wu, M. She, et al., Novel fluorescein-based fluorescent probe for detecting H_2S and its real applications in blood plasma and biological imaging, *Anal. Chem.* 88 (2016) 11253–11260.
- [9] B.S. Kasinath, D. Feliers, H.J. Lee, Hydrogen sulfide as a regulatory factor in kidney health and disease, *Biochem. Pharmacol.* 149 (2018) 29–41.
- [10] K. Li, F. Chen, Q. Yin, et al., A colorimetric and near-infrared fluorescent probe for hydrogen polysulfides and its application in living cells, *Sensors Actuators B Chem.* 254 (2018) 222–226.
- [11] C. Zhan, G. Zhang, D. Zhang, Zincke's salt-substituted tetraphenylethylenes for fluorometric turn-on detection of glutathione and fluorescence imaging of cancer cells, *ACS Appl. Mater. Interfaces* 10 (2017) 12141–12149.
- [12] D. Gong, J. Ru, T. Cao, et al., Two-stage ratiometric fluorescent responsive probe for rapid glutathione detection based on BODIPY thiol-halogen nucleophilic mono- or disubstitution, *Sensors Actuators B Chem.* 258 (2018) 72–79.
- [13] W. Niu, L. Guo, Y. Li, et al., Highly selective two-photon fluorescent probe for ratiometric sensing and imaging cysteine in mitochondria, *Anal. Chem.* 88 (2016) 1908–1914.
- [14] X. Xie, C. Yin, Y. Yue, et al., Fluorescent probe detect distinguishly sulfide/hydrogen sulfide and thiol via two emission channels in vivo, *Sensors Actuators B Chem.* 277 (2018) 647–653.
- [15] S. Cai, C. Liu, X. Jiao, et al., A lysosome-targeted near-infrared fluorescent probe for imaging endogenous cysteine (Cys) in living cells, *J. Mater. Chem. B* 8 (2020) 2269–2274.
- [16] J.O. Escobedo, W. Wang, R.M. Strongin, Use of a commercially available reagent for the selective detection of homocysteine in plasma, *Nat Pro* 1 (2006) 2759–2762.
- [17] Y. Xia, H. Zhang, X. Zhu, et al., A highly selective two-photon fluorescent chemosensor for tracking homocysteine via situ reaction, *Dyes Pigments* 155 (2018) 159–163.
- [18] D. Chen, Z. Long, Y. Sun, et al., A red-emission probe for intracellular biothiols imaging with a large Stokes shift, *J. Photochem. and Photobio. A Chem.* 368 (2018) 90–96.
- [19] D. Li, J. Zhang, J. Cui, et al., A ratiometric fluorescent probe for fast detection of hydrogen sulfide and recognition of biological thiols, *Sensors Actuators B Chem.* 234 (2016) 231–238.
- [20] P. Bhattacharjee, S. Chatterjee, A. Achari, et al., A bis-indole/carbazole based C5-curcuminoid fluorescent probe with large Stokes shift for selective detection of biothiols and application to live cell imaging, *Analyst* 145 (2020) 1184–1189.
- [21] Y. Yang, Y. Wang, Y. Feng, et al., Light-driven visualization of endogenous cysteine, homocysteine, and glutathione using a near-infrared fluorescent probe, *J. Mater. Chem. B* 7 (2019) 7723–7728.

- [22] E. Mattiussi, N. Kaminari, M. Ponte, H. Ponte, Behavior analysis of a porous bed electrochemical reactor the treatment of petrochemical industry wastewater contaminated by hydrogen sulfide (H₂S), *Chem. Eng. J.* 275 (2015) 305–314.
- [23] Q. Zhang, Determination of H₂S in gas by colorimetry of isonicotinic acid and pyrazolone, *Fuel Chem. Pro.* 35 (2014) 32–34.
- [24] P. Hou, J. Sun, H. Wang, et al., TCF-imidazo[1,5- α]pyridine: a potential robust ratiometric fluorescent probe for glutathione detection with high selectivity, *Sensors Actuators B Chem.* 304 (2020) 127244–127250.
- [25] Y. Cai, J. Fang, H. Zhu, et al., A rapid “off-on” copper-induced AIE active sensor for fluorimetric detection of cysteine, *Sensors Actuators B Chem.* 303 (2020) 127214–127221.
- [26] V.K. Gupta, Electrocatalytic determination of L-cysteine in the presence of tryptophan using carbon paste electrode modified with MgO nanoparticles and acetylferrocene, *Int. J. Electrochem. Sci.* 5 (2018) 4309–4318.
- [27] X. Chen, Y. Zhou, X. Peng, et al., Fluorescent and colorimetric probes for detection of thiols, *Chem. Soc. Rev.* 39 (2010) 2120–2135.
- [28] H.S. Jung, X. Chen, J.S. Kim, et al., Recent progress in luminescent and colorimetric chemosensors for detection of thiols, *Chem. Soc. Rev.* 42 (2013) 6019–6031.
- [29] H. Zeng, Z. Zhou, F. Liu, et al., Design and synthesis of a vanadate-based ratiometric fluorescent probe for sequential recognition of Cu²⁺ ions and biothiols, *Analyst* 144 (2019) 7368–7377.
- [30] L. Yuan, W. Lin, S. Zhao, et al., A unique approach to development of near-infrared fluorescent sensors for in vivo imaging, *J. Am. Chem. Soc.* 134 (2012) 13510–13523.
- [31] L. Fan, W. Zhang, X. Wang, et al., A two-photon ratiometric fluorescent probe for highly selective sensing of mitochondrial cysteine in live cells, *Analyst* 144 (2019) 439–447.
- [32] B. Peng, W. Chen, C. Liu, et al., Fluorescent probes based on nucleophilic substitution-cyclization for hydrogen sulfide detection and bioimaging, *Chem. Eur. J.* 20 (2014) 1010–1016.
- [33] J. Zhang, B. Yu, L. Ning, et al., A near-infrared fluorescence probe for thiols based on analyte-specific cleavage of carbamate and its application in bioimaging, *Eur. J. Org. Chem.* 2015 (2015) 1711–1718.
- [34] S. Chen, P. Hou, J. Wang, et al., A highly sensitive fluorescent probe based on the Michael addition mechanism with a large Stokes shift for cellular thiols imaging, *Anal. Bioanal. Chem.* 410 (2018) 4323–4330.
- [35] Y. Wang, L. Yang, X. Wei, et al., Fluorescent probe based on rosamine with pyridinium unit for hydrogen sulfide detection in mitochondria, *Anal. Methods* 10 (2018) 5291–5296.
- [36] E. Zaorska, M. Konop, R. Ostaszewski, M. Ufnal, et al., Salivary hydrogen sulfide measured with a new highly sensitive self-immolative coumarin-based fluorescent probe, *Molecules* 23 (2018) 2241–2256.
- [37] J. Wang, Y. Wen, F. Huo, et al., Based ‘successive’ nucleophilic substitution mitochondrial-targeted H₂S red light emissive fluorescent probe and its imaging in mice, *Sensors Actuators B Chem.* 297 (2019) 126773–126779.
- [38] X. Xia, Y. Qian, NIR two-photon fluorescent probe for biothiol detection and imaging of living cells in vivo, *Analyst* 143 (2018) 5218–5224.
- [39] X. Jin, X. Sun, X. Di, et al., Novel fluorescent ESIPT probe based on flavone for nitroxyl in aqueous solution and serum, *Sensors Actuators B Chem.* (2016) 209–216.
- [40] M. Tian, J. Sun, Y. Tang, et al., Discriminating live and dead cells in dual-color mode with a two-photon fluorescent probe based on ESIPT mechanism, *Anal. Chem.* 90 (2017) 998–1005.
- [41] X. Jin, L. Dong, X. Di, et al., NIR luminescence for the detection of latent fingerprints based on ESIPT and AIE processes, *RSC Adv.* 5 (2018) 87306–87310.
- [42] X. Jin, C. Liu, X. Wang, et al., A flavone-based ESIPT fluorescent sensor for detection of N₂H₄ in aqueous solution and gas state and its imaging in living cells, *Sensors Actuators B Chem.* 216 (2015) 141–149.
- [43] B. Liu, H. Wang, T. Wang, et al., A new ratiometric ESIPT sensor for detection of palladium species in aqueous solution, *Chem. Commun.* 48 (2012) 2867–2869.
- [44] L.K. Kumawat, M. Asif, V.K. Gupta, Dual ion selective fluorescence sensor with potential applications in sample monitoring and membrane sensing, *Sensors Actuators B Chem.* 241 (2017) 1090–1098.
- [45] Z. Song, R.T.K. Kwok, E. Zhao, et al., A ratiometric fluorescent probe based on ESIPT and AIE processes for alkaline phosphatase activity assay and visualization in living cells, *ACS Appl. Mater. Interfaces* 6 (2014) 17245–17254.
- [46] A. Halith, T. Sivakumar, Synthesis and chemical characterisation of some novel substituted flavone's for it's anti microbial activity, *Int. J. Curr. Pharm. Res.* 1 (2011) 497–505.
- [47] I. Serdiuk, M. Reszka, B. Liberek, et al., Determination of low-activity hydrolases using ESIPT fluorescent indicators on silver surfaces, *Dyes Pigments* 149 (2018) 149224–149228.
- [48] V.K. Gupta, N. Mergu, L.K. Kumawat, Y. Qi, M. Lu, Y. Wang, et al., Selective naked-eye detection of magnesium (II) ions using a coumarin-derived fluorescent probe, *Sensors Actuators B Chem.* 207 (2015) 216–223.
- [49] V.K. Gupta, N. Mergu, L.K. Kumawat, A new multifunctional rhodamine-derived probe for colorimetric sensing of Cu(II) and Al(III) and fluorometric sensing of Fe(III) in aqueous media, *Sensors Actuators B Chem.* 223 (2016) 101–113.
- [50] V.K. Gupta, A.K. Singh, L.K. Kumawat, Thiazole Schiff base turn-on fluorescent chemosensor for Al³⁺ ion, *Sensors Actuators B Chem.* 195 (2014) 98–108.
- [51] V.K. Gupta, A.K. Singh, L.K. Kumawat, et al., An easily accessible switch-on optical chemosensor for the detection of noxious metal ions Ni(II), Zn(II), Fe(III) and UO₂(II), *Sensors Actuators B Chem.* 222 (2016) 468–482.
- [52] M. Lan, J. Wu, W. Liu, et al., Highly sensitive fluorescent probe for thiols based on combination of PET and ESIPT mechanisms, *Sensors Actuators B Chem.* 156 (2011) 332–337.
- [53] Y. Ji, L. Xia, L. Chen, et al., A novel BODIPY-based fluorescent probe for selective detection of hydrogen sulfide in living cells and tissues, *Talanta* 181 (2018) 104–111.
- [54] R. Sung, K. Sung, TICT excited states of o- and p-N,N-dimethylamino analogues of GFP chromophore, *J. Phys. Org. Chem.* 31 (2018) 3791–3798.
- [55] Y. Qi, M. Lu, Y. Wang, et al., A theoretical study of the ESIPT mechanism of 3-hydroxyflavone derivatives: solvation effect and the importance of TICT for its dual fluorescence properties, *Org. Chem. Front* 6 (2019) 3136–3143.
- [56] Y. Chen, Y. Piao, X. Feng, et al., Excited state intramolecular proton transfer (ESIPT) luminescence mechanism for 4-N,N-diethylamino-3-hydroxyflavone in propylene carbonate, acetonitrile and the mixed solvents, *Spectrochim. Acta A* 224 (2020) (117416–117411).